Available online at www.sciencedirect.com

ScienceDirect

IFAC Papers Online CONFERENCE PAPER ARCHIVE

IFAC PapersOnLine 53-2 (2020) 15699–15704

Vehicular Lateral Tracking Control with Winding Road Disturbance Compensation

Woo Young Choi * **Seung-Hi Lee** ** **Chung Choo Chung** ***

* *Dept. of Electrical Engineering, Hanyang University, Seoul 04763, South Korea. (e-mail: wooyoungchoi@hanyang.ac.kr)*
** *Dept. of Mechanical and System Design Engineering, Hongik University, Seoul 04066, South Korea. (e-mail: shlee@ieee.org)*
*** *Div. of Electrical and Biomedical Engineering, Hanyang University, Seoul 04763, South Korea. (e-mail: cchung@hanyang.ac.kr)*

Abstract: In this paper, an innovative vehicular lateral tracking control scheme is proposed to compensate for a winding road disturbance (WRD) on a curved road. Using a dynamic lateral motion model with look-ahead distance, we propose a WRD compensator (WRDC) to sufficiently achieve satisfactory vehicular lateral tracking control performance on the curved road in the presence of WRD. The proposed tracking control scheme is designed by the WRDC gain from the dominant state for the lateral offset in the lane keeping control. By developing the WRDC, state-space reference is redesigned to compensate for tracking error. We showed that the proposed WRDC ensures that the projected tracking error converges to zero. To verify the usefulness of the tracking control, the WRDC applied to a linear quadratic regulator (LQR) controller was compared to the standard LQR, LQR with an integrator, and LQR with an anti-windup. We observed that the proposed WRDC is not only robust against road curvature variation but also outperforming the tracking performance of LQR with anti-windup.

Keywords: Autonomous Driving, Lateral Control, Lane Keeping System, Curved Road, External Disturbance, Anti-windup, Unmatched Disturbance

NOMENCLATURE

$\{XYZ\}$	Global coordinate frame
$\{xyz\}$	Vehicle coordinate frame
x	Front fixed longitudinal position in $\{xyz\}$
y	Lateral position of the origin of $\{xyz\}$ to the center of turn (CT).
ψ	Yaw, heading angle of vehicle in global axis
$\dot{\psi}$	Yaw rate of vehicle
V_x (V_y)	Longitudinal (lateral) velocity at the center of gravity (CG) of vehicle
m	Total mass of vehicle
I_z	Yaw moment of inertia of vehicle
l_f (l_r)	Longitudinal distance from CG to front (rear) tires
l_{fr}	$l_f + l_r$, Wheelbase
α_f (α_r)	Slip angle at front (rear) wheel tires
$C_{\alpha f}$ ($C_{\alpha r}$)	Cornering stiffness of front (rear) tires
δ	Steering angle
F_{yf} (F_{yr})	Lateral tire force on front (rear) tires
e_y	$y - y^d$, Lateral position error w.r.t. reference
$\dot{e}_y$	$\dot{y} - \dot{y}^d$, Time derivative of lateral position error w.r.t. reference
e_ψ	$\psi^d - \psi$, Yaw angle error w.r.t. reference
e_{yL}	$y_L - y_L^d$, Lateral position error at look-ahead point
L	Look-ahead distance from c.g. to look-ahead point

SUPERSCRIPTS

d	Desired

1. INTRODUCTION

Vehicular tracking control issues of autonomous vehicles for advanced driver assistance systems (ADASs) have been actively studied in the automotive industry. These vehicular tracking control technologies in ADASs such as lane keeping system (LKS) and waypoint tracking control are expected to enhance driving safety and to reduce the driver workload, thus reducing the risk of accidents. However, the tracking control is affected by external disturbances depending on a road curvature, such as curved roads. The external disturbances of vehicle models cause lateral position errors in the LKS on the curved roads. In this regard, the lateral offset increased depending on the road curvature Kang et al. (2018). Tracking controls using robust H_∞ output-feedback control strategy Hu et al. (2016) and model predictive control (MPC) Choi et al. (2018) were tested in curved road scenarios. In Choi et al. (2017), the lateral offset occurred despite the use of horizon-wise constant MPC (HWC MPC) considering vehicle speed variation parameter in waypoint tracking on the curved road. The lateral offset also occurred in vision-based LKS Tunçer et al. (2010). These external disturbances of LKS on the curved roads can adversely affect driving safety.

Various techniques have been used to reduce the lateral position error on the curved roads. In Son et al. (2015), the authors verified that the integrator with a predictive virtual lane can be used to reduce the lateral position error on the curved

⋆ This work was supported by the Industrial Source Technology Development Programs (No.10082585, Development of deep learning-based open EV platform technology capable of autonomous driving), and (No.10076707, AI-based driving risk assessment and optimal ADAS/chassis control) funded by the Ministry of Trade, Industry and Energy (MOTIE, Korea).

10.1016/j.ifacol.2020.12.2565

road. This integrator method significantly reduced the lateral position error. In other ways, the authors applied H_∞ control in path-tracking applications to reduce the tracking error on curved roads Park et al. (2018). In Lin et al. (2000), the authors proposed a path prediction algorithm that includes a linearized path projection model and an external disturbance characterization scheme. In Boudali et al. (2019), the authors proposed a unified lateral guidance approach to deal with the discontinuous reference trajectory. In Kim et al. (2019), the deep neural network (DNN) was applied to LKS on curved roads to reduce unmatched disturbance. In Kim et al. (2018), the sliding surface was designed to reduce the unmatched disturbance in LKS, but the unmatched disturbance could not be completely removed.

Using simple integral action may becomes very dangerous in real autonomous driving situations for example such as temporary failure of a camera sensor. An Anti-windup compensator for integral action may partially resolve the problem of the integrator Åström and Rundqwist (1989); Kothare et al. (1994). In Johnson (1971), the authors described a simple case where the external disturbance occurs with a priory known waveform. A leader-follower consensus tracking problem for multi-agent systems with identical general linear dynamics and unknown external disturbances was solved by consensus algorithm based on state and disturbance estimates Cao et al. (2015). In Van Loon et al. (2014), the authors presented the split-path nonlinear integrator (SPANI) as a novel nonlinear filter designed to improve the transient performance of linear systems.

In this paper, we develop a robust tracking control scheme with winding road disturbance (WRD) compensation for autonomous driving. To achieve sufficient vehicular lateral tracking control performance on the curved road in the presence of WRD, this paper designs a scheme of WRD compensation. In developing a robust tracking control against WRD, the proposed WRD compensation scheme develops a state-space reference redesign technique. We will also demonstrate the utility of the proposed WRD compensator (WRDC) by application test with experiment data.

2. ROAD AND VEHICLE MODEL

To begin with, let's introduce a brief review of a clothoid road model and a vehicle lateral motion model.

2.1 Road Model

In this section, we use a cubic polynomial curve for a road model. From the lane information of road, the lane polynomial $f(x)$ is defined as a cubic polynomial function of the longitudinal distance x.

$$f(x) = c_0 + c_1 \cdot x + c_2 \cdot x^2 + c_3 \cdot x^3 \tag{1}$$

here c_0 is the lateral offset, c_1 is the heading angle, $2c_2$ is the curvature, and $6c_3$ is the curvature rate. The clothoid cubic polynomial with a clothoid constraint is used to create these curves (see Kang et al. (2014); Lee and Chung (2016)). The lane polynomial is mainly obtained by a camera or global positioning system (GPS) sensor. The camera sensor can detect lanes based on vehicle coordinates, and GPS can detect lane maps and vehicle coordinates from global positions. The lane polynomial is fixed until the next lane information arrives from either a camera or a GPS system, while the vehicle trajectory

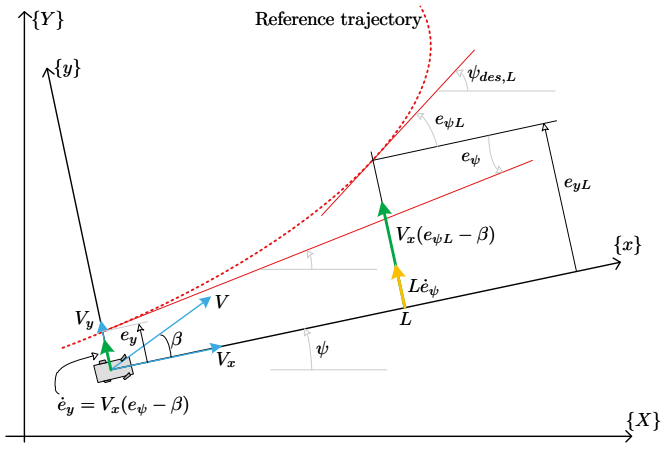

Fig. 1. Lateral motion with look-ahead distance.

is solely determined by the vehicle's momentum, such as its velocity and yaw rate.

2.2 Dynamic Lateral Motion Model

We use a vehicle dynamic lateral motion model with a look-ahead distance being considered as shown in Fig. 1. The look-ahead distance L is introduced to mimic human drivers' driving behavior. The lateral dynamic model on the error terms at the look-ahead distance is derived as follows Son et al. (2015); Lee and Chung (2016)

$$\dot{\mathbf{x}} = \underbrace{\begin{bmatrix} 0 & 1 & 0 & -L \\ 0 & a_{22} & a_{23} & a'_{24} \\ 0 & 0 & 0 & -1 \\ 0 & a'_{42} & a_{43} & a_{44} \end{bmatrix}}_{A} \mathbf{x} + \underbrace{\begin{bmatrix} 0 \\ b'_{21} \\ 0 \\ b_{41} \end{bmatrix}}_{B} \mathbf{u} + \underbrace{\begin{bmatrix} L & V_x \\ V_x & 0 \\ 1 & 0 \\ 0 & 0 \end{bmatrix}}_{B_\varphi} \varphi \tag{2}$$

with the state vector $\mathbf{x} = \begin{bmatrix} e_{yL} & \dot{e_y} & e_\psi & \dot{\psi} \end{bmatrix}^T$, the control input $\mathbf{u} = \delta$ and winding road disturbance (WRD) $\varphi = \begin{bmatrix} \dot{\psi}^d \\ e_{\psi L} - e_\psi \end{bmatrix}$, where

$$a_{22} = -\frac{2C_{\alpha f} + 2C_{\alpha r}}{mV_x},\ a_{23} = -a_{22}V_x,$$
$$a_{24} = -1 - \frac{2C_{\alpha f}l_f - 2C_{\alpha r}l_r}{mV_x{}^2},\ a'_{24} = (a_{24} - 1)V_x,$$
$$a_{42} = -\frac{2C_{\alpha f}l_f - 2C_{\alpha r}l_r}{I_z},\ a'_{42} = a_{42}/V_x,$$
$$a_{43} = -a_{42},\ a_{44} = -\frac{2C_{\alpha f}l_f{}^2 + 2C_{\alpha r}l_r{}^2}{I_z V_x},$$
$$b_{21} = \frac{2C_{\alpha f}}{mV_x},\ b'_{21} = b_{21}V_x,\ b_{41} = \frac{2C_{\alpha f}l_f}{I_z}.$$

The zero-order hold (ZOH) discrete-time equivalent model $(\Phi, \Gamma, \Gamma_\varphi)$ for a given sampling period T_c to (A, B, B_φ) is given by

$$\mathbf{x}(k+1) = \Phi\mathbf{x}(k) + \Gamma\mathbf{u}(k) + \Gamma_\varphi\varphi(k), \tag{3}$$

where

$$\Phi = e^{AT_c}, \Gamma = \int_0^{T_c} e^{A(T_c-\tau)}Bd\tau, \Gamma_\varphi = \int_0^{T_c} e^{A(T_c-\tau)}B_\varphi d\tau. \tag{4}$$

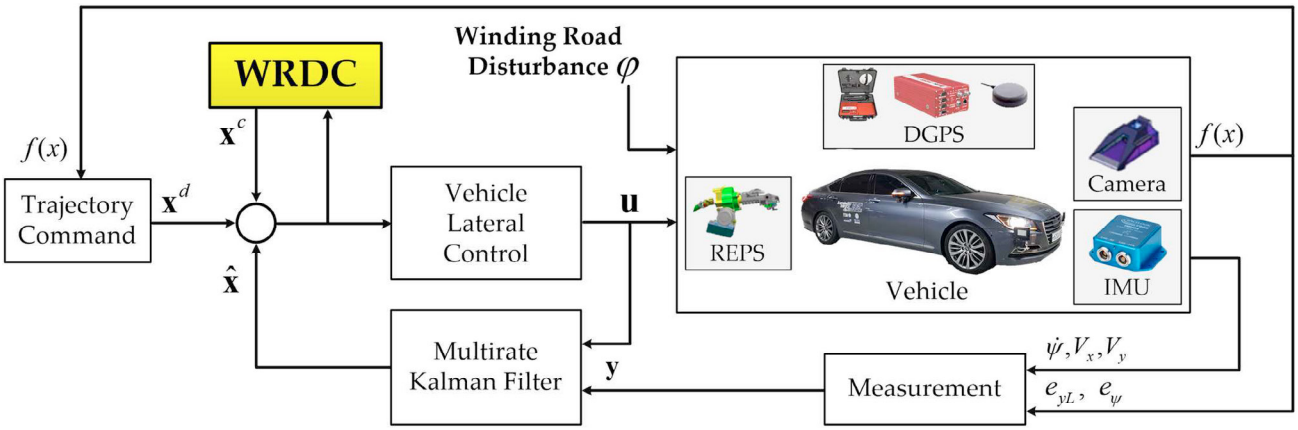

Fig. 2. Overall process with the winding road disturbance compensator (WRDC).

3. TRACKING CONTROL WITH WINDING ROAD DISTURBANCE COMPENSATION

For the tracking control configuration, let $\mathbf{x}^d$ be the state reference for road, and $\mathbf{y}$ be the output states for the dynamic lateral motion model. As shown in Fig. 2, $\mathbf{x}^d$ is provide from the trajectory command and $\mathbf{y}$ can be obtained from the vehicle environment sensors and inertial measurement unit (IMU). The estimated state of (2) $\hat{\mathbf{x}}$ can be calculated from the multirate Kalman filter taking into account the different update periods of the sensors Son et al. (2015); Lee and Chung (2016). Let us assume that the state-feedback controller is given by

$$\mathbf{u}(k) = -K(\mathbf{x}^d(k) - \hat{\mathbf{x}}(k)) \tag{5}$$

where K is the control gain. The desired state values, $\mathbf{x}^d$ for (2) can be obtained using the following equations Lee and Chung (2016):

$$\begin{aligned} e^d_{yL} &= f(L) = c_0 + c_1 L + c_2 L^2 + c_3 L^3, \\ \dot{e}^d_y &= -\nu c_0, \\ e^d_{\psi} &= 0, \\ \dot{\psi}^d &= 0. \end{aligned} \tag{6}$$

where some real value $\nu > 0$. As an example of a simple state-feedback controller, a linear quadratic regulator (LQR) (see Ji and Chizeck (1990) for controllability) is used for the lane keeping control. To obtain optimal control gain K, we minimize the linear quadratic cost function

$$J = \sum_{k=0}^{\infty} (\mathbf{x}(k)^T Q \mathbf{x}(k) + \mathbf{u}(k)^T R \mathbf{u}(k)) \tag{7}$$

by solving the discrete-time algebraic Riccati equation (DARE). where Q and R are weighting coefficient.

Applying lane tracking control such as state feedback exhibits lateral offset on the curved road due to the problematic WRD φ that always appears unless the road has zero curvature. The tracking error is caused by the WRD φ in equation (8). Utilizing the coefficients c_2 and c_3 in the road lane curve $f(x)$, we can calculate WRD φ as follows:

$$\varphi = \begin{bmatrix} \dot{\psi}^d \\ e_{\psi L} - e_{\psi} \end{bmatrix} = \begin{bmatrix} 2V_x & 0 \\ 2L & 3L^2 \end{bmatrix} \begin{bmatrix} c_2 \\ c_3 \end{bmatrix}. \tag{8}$$

This WRD includes the matched as well as unmatched disturbances. Compensation becomes more difficult if it includes an unmatched disturbance. Therefore, we need to develop an effective scheme to compensate the effect of WRD.

Here, we propose a WRD compensator (WRDC). Our innovative approach is to apply a redesign of the state reference $\mathbf{x}^d$ such that $\mathbf{x}^d + \mathbf{x}^c$ enforces accurate tracking of $\mathbf{x}^d$. The goal is to reduce the tracking error $\mathbf{x}^d(k) - \hat{\mathbf{x}}(k)$ to zero. Therefore, we modify the state reference $\mathbf{x}^d(k)$ using additional $\mathbf{x}^c(k)$ such that the WRD compensator (WRDC) becomes

$$\mathbf{u}(k) = -K(\mathbf{x}^d(k) + \mathbf{x}^c(k) - \hat{\mathbf{x}}(k)) \tag{9}$$

with a hope to attain

$$\Gamma K \mathbf{x}^c(k) \approx -\Gamma_{\varphi} \varphi(k). \tag{10}$$

However, $\mathbf{x}^c$ cannot be computed form (10), because ΓK is usually singular. Further, Γ and Γ_{φ} show different domain and range such that a control equivalent term to compensate for WRD cannot work. In other word, the WRD includes unmatched disturbance. Therefore, we propose a WRDC scheme:

$$\mathbf{x}^c(k) := \text{sat}[\Omega(\mathbf{x}^d(k-1) + \mathbf{x}^c(k-1) - \hat{\mathbf{x}}(k-1))] \tag{11}$$

where sat$(\cdot)$ is an element-wise saturation function that bounds a pre-specified value $\pm \mathbf{x}^c_{\text{max}}$ (For example, lane width in lane keeping control). By redesigning the state-space reference, we are to remove the tracking error $\mathbf{x}^d(k) - \hat{\mathbf{x}}(k)$. We design a WRDC gain Ω such that

$$\begin{aligned} \Gamma K \mathbf{x}^c(k) &= \Gamma K \Omega(\mathbf{x}^d(k-1) + \mathbf{x}^c(k-1) - \hat{\mathbf{x}}(k-1)) \\ &\approx -\Gamma_{\varphi} \varphi(k) \end{aligned} \tag{12}$$

When there is no excessive compensation, (12) is satisfied, otherwise the sat$(\cdot)$ is activated. The WRDC gain $\Omega \in \mathbb{R}^{4\times 4}$ can be designed from dominant states for lateral position error e_y in lane keeping control. Determining $\mathbf{x}^c$ with a larger range allows effective compensation of WRD that includes matched as well as unmatched components. We can achieve state-space tracking control with WRD compensation by state-space reference redesign producing

$$\begin{aligned} \mathbf{x}(k+1) &= \Phi \mathbf{x}(k) + \Gamma K(\mathbf{x}^d(k) + \mathbf{x}^c(k) - \hat{\mathbf{x}}(k)) + \Gamma_{\varphi} \varphi \\ &\approx \Phi \mathbf{x}(k) + \Gamma K(\mathbf{x}^d(k) - \hat{\mathbf{x}}(k)). \end{aligned} \tag{13}$$

It should be noted that the redesign term $\mathbf{x}^c$ contributes to attaining accurate tracking by removing any tracking error.

Now, we take a closer look at the stability of WRDC.

Lemma 1. Given Ω satisfying $\|\Omega\| < 1$, there exists some $0 < \rho < 1$, such that $\mathbf{x}^c(\cdot)$ is a sequence satisfying

$$\|\mathbf{x}^c(k) - \Omega(k)\mathbf{x}^c(k-1)\| \leq \rho \|\mathbf{x}^c(k-1)\|. \tag{14}$$

◇

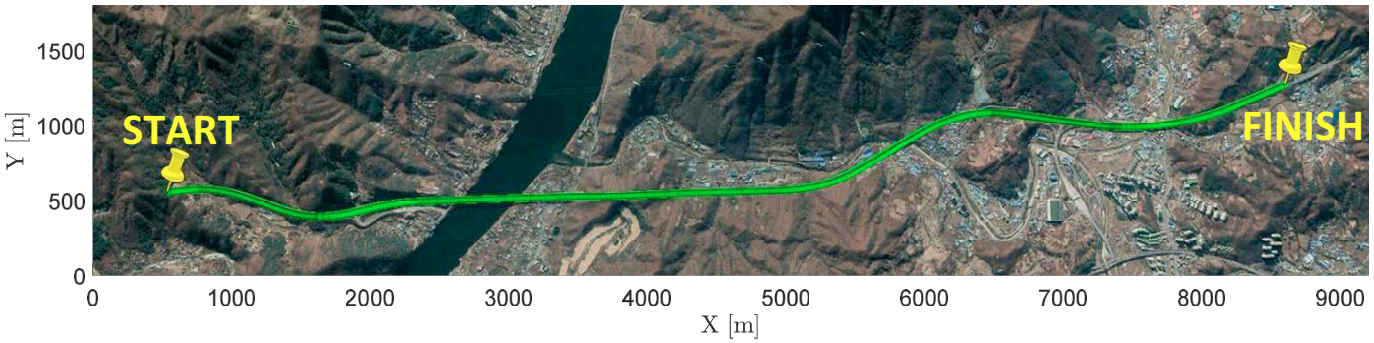

Fig. 3. Curved road: Seoul-Yangyang expressway 60 in Korea.

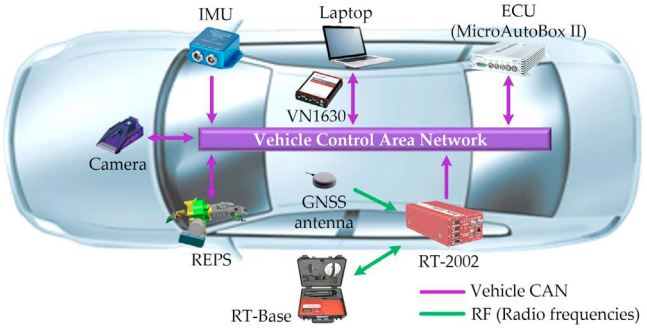

Fig. 4. Experimental environment setup.

Proof. Given Ω satisfying $\|\Omega\| < 1$, there exist some $0 < \acute{\rho} < 1$ such that $\mathbf{x}^c(k) = \Omega\mathbf{x}^c(k-1) + \acute{\rho}\mathbf{x}^c(k-1)$ be convergent. Then, it is immediate to find

$$\|\mathbf{x}^c(k) - \Omega\mathbf{x}^c(k-1)\| \leq \rho\|\mathbf{x}^c(k-1)\|, \quad \text{for } 0 < \acute{\rho} < \rho < 1. \tag{15}$$

This completes the proof. ■

The Lemma 1 is to state the existence of $0 < \rho < 1$ for the convergent sequence $\mathbf{x}^c(\cdot)$.

Proposition 1. Suppose that the stable closed-loop system described by Ω is tracking a state reference $\mathbf{x}^d(\cdot)$. Applying a state reference redesign $\mathbf{x}^d(k) + \mathbf{x}^c(k)$, with

$$\mathbf{x}^c(k) = \Omega(\mathbf{x}^d(k-1) + \mathbf{x}^c(k-1) - \hat{\mathbf{x}}(k-1)) \tag{16}$$

and the condition $\|\mathbf{x}^c(k) - \Omega\mathbf{x}^c(k-1)\| \leq \rho\|\mathbf{x}^c(k-1)\|$ in (14) being satisfied, assures that $\|\mathbf{x}^c(k) - \Omega\mathbf{x}^c(k-1)\| = \|\Omega(\mathbf{x}^d(k-1) - \hat{\mathbf{x}}(k-1))\|$. Further, the projected tracking error $\|\Omega(\mathbf{x}^d(\cdot) - \hat{\mathbf{x}}(\cdot))\|$ converges to zero as ρ converges to zero. ◇

Proof. Proof immediately comes from the application of the Lemma 1. With the condition (14) being satisfied, the sequence $\mathbf{x}^c(\cdot)$ is convergent and the sequence $\mathbf{x}^c(k) - \Omega\mathbf{x}^c(k-1)$ is also convergent. From equation (16), we rewrite it as

$$\mathbf{x}^c(k) - \Omega\mathbf{x}^c(k-1) = \Omega(\mathbf{x}^d(k-1) - \hat{\mathbf{x}}(k-1)), \tag{17}$$

it is immediate from Lemma 1 to find that

$$\begin{aligned} &\|\Omega(\mathbf{x}^d(k-1) - \hat{\mathbf{x}}(k-1))\| \\ &= \|\mathbf{x}^c(k) - \Omega\mathbf{x}^c(k-1)\| \leq \rho\|\mathbf{x}^c(k-1)\| \end{aligned} \tag{18}$$

converges to zero as ρ converges to zero. ■

Corollary 1. Proposition 1 applies for a state reference redesign $\mathbf{x}^d(k) + \mathbf{x}^c(k)$ with

$$\mathbf{x}^c(k) = \text{sat}[\Omega(\mathbf{x}^d(k-1) + \mathbf{x}^c(k-1) - \hat{\mathbf{x}}(k-1))] \tag{19}$$

form condition (11). ◇

Proof. Proof comes directly from

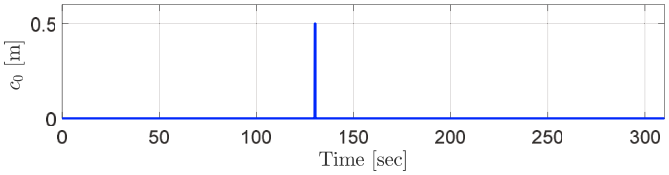

Fig. 5. Transient disturbance for lateral position error: we applied impulse disturbances of 0.5 m to the c_0 value of the camera sensor for one sampling period T_c at 130 sec.

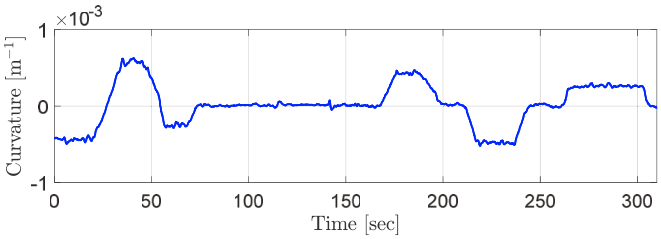

Fig. 6. Road curvature measured by camera (Mobileye) sensor.

$$\begin{aligned} &\|\Omega(\mathbf{x}^d(k-1) - \hat{\mathbf{x}}(k-1))\| \\ &= \|\mathbf{x}^c(k) - \Omega\mathbf{x}^c(k-1)\| \leq \rho\|\mathbf{x}^c(k-1)\| \leq \rho\|\mathbf{x}^c_{\max}\| \end{aligned} \tag{20}$$

and the result of Proposition 1 in (18). ■

4. APPLICATION RESULTS

In this section, we describe how useful the proposed WRDC is in lane keeping control on the curved road.

4.1 Experimental Setup

To set up the experiment, vehicle and camera (Mobileye) data are given by the vehicle driven by a human driver on the Seoul-Yangyang expressway in Korea as shown in Fig. 3. Vehicle data was obtained using a passenger car GENESIS from Hyundai Motors. The vehicle speed was about 80 km/h. The vehicle and sensors data were collected via dSPACE MicroAutoBox II, analyzed with Vector's CANoe with VN1630, and evaluated using MATLAB/Simulink in Fig. 4. To show the winding road, the differential GPS (DGPS) data is collected at an update period of 10 ms from OxTS (global navigation satellite system (GNSS) antenna, RT-2002 and RT-Base) with its real time kinematic (RTK) positioning service (1σ = 0.01 m) in Fig. 3.

4.2 Experimental Condition

To confirm the performance of the proposed method, the experiment of the tracking control was performed through simulations with real road data obtained by a camera sensor. For

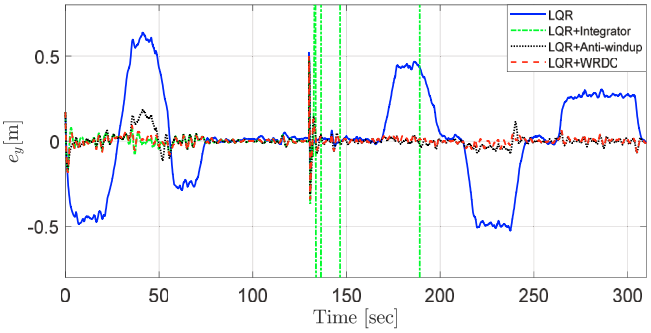

Fig. 7. Lateral position error e_y.

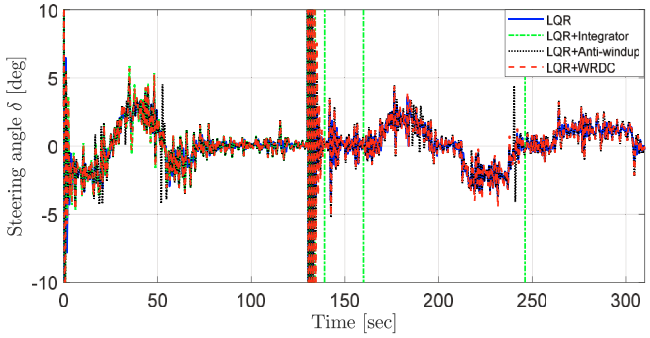

Fig. 8. Steering angle δ.

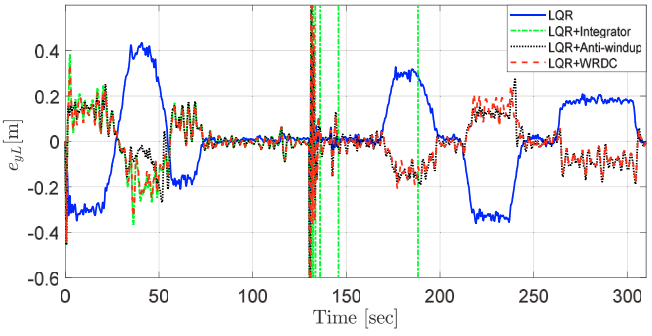

Fig. 9. Lateral position error at look-ahead point e_{yL}.

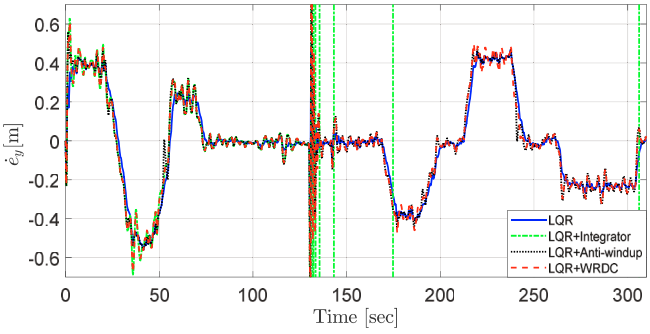

Fig. 10. Time derivative of lateral position error $\dot{e}_y$.

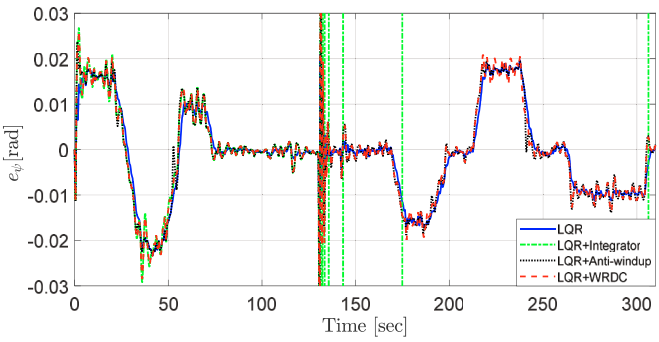

Fig. 11. Yaw angle error e_ψ.

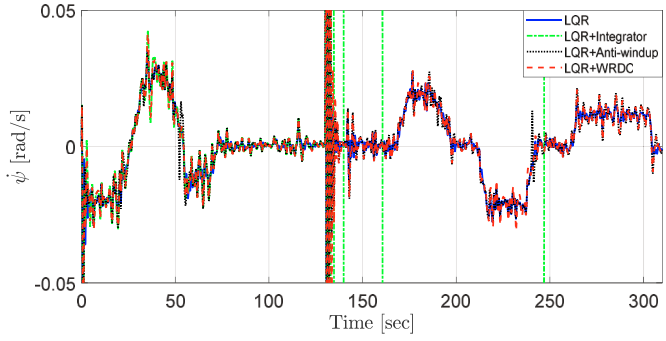

Fig. 12. Yaw rate $\dot{\psi}$.

performance comparison, we applied the transient (impulse) disturbances of 0.5 m to the c_0 value of the camera sensor for one sampling period T_c at 130 sec as shown in Figs. 5 and 6. This assumes momentary sensor failure and incorrect information. Figure 6 shows the road curvature measured by the camera sensor. here, the curved road is about 0 to 75 sec and 170 to 300 sec and the straight road is 75 to 170 sec.

To verify the utility of the proposed reference redesign method, we designed the standard LQR calculated by equation (9), and the integrator from the state-feedback of the dominant state for lateral position error c_0 computed by a camera sensor. In addition, anti-windup is designed to resolve the transient disturbance vulnerability of the integrator Åström and Rundqwist (1989); Kothare et al. (1994). We verified the usefulness of the proposed method by comparing the four methods. Here, the look-ahead distance L is 20 m, the sampling period T_c is 10 ms, and the vehicle speed used in the experiment is a constant 80 km/h.

4.3 Experiment Results

The lateral position error e_y is dramatically reduced by the proposed method, as shown in Fig. 7. In lane keeping control application, the LQR controller increased the lateral position error by the curvature of the curved section. This is because WRD exists on curve roads. The lateral position error in the curved section can be reduced using an integrator, but it is diverged at 130 sec by impulse disturbance because the integrator has a weakness for the transient disturbance. This controller is dangerous in real autonomous driving situations (for example momentary camera sensor failure and incorrect information). To resolve this problem, we applied the anti-windup method. The anti-windup method was robust for impulse disturbance at 130 sec. However, anti-windup has not been able to compensate for the lateral position error more than the integrator on sharp curve roads about 35 to 40 sec. This is due to the saturation of the anti-windup. Compared to these methods, the proposed WRDC method dramatically compensates for lateral position error e_y. In this regard, the steering angle and vehicle states showed in Figs. 8 to 12. In Fig. 9, the integrator, anti-windup, and WRDC showed signs ($+$ or $-$) opposite of LQR on the curved road because the vehicles of these methods are in the center of the road. The proposed WRDC method dramatically reduced the lateral offset as shown in Fig. 13 The standard LQR showed that lateral position error occurs depending on the road curvature. This was due to the WRD φ calculated

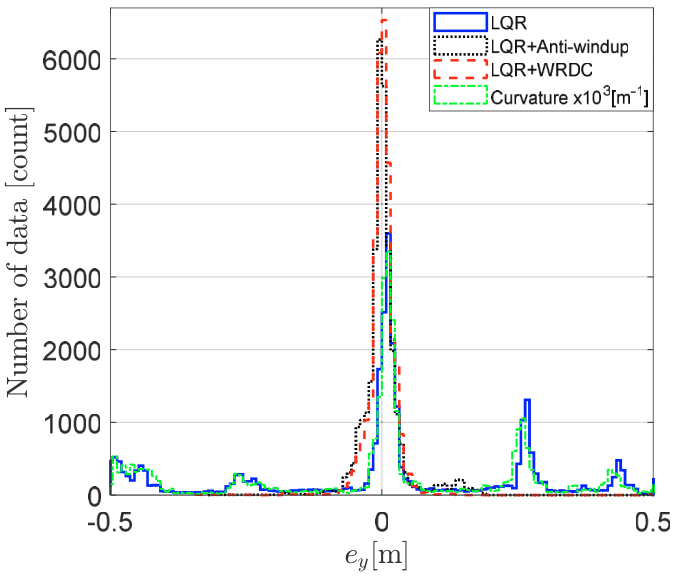

Fig. 13. Histogram of lateral offset e_y.

by the road curvature. Thus, by comparing the curvature and LQR, we can observe the lateral position error dependent on the road curvature. The anti-windup works well on a road with small curvature but it does not effectively compensate for the large curvature road. Notice that the integrator was not been shown in Fig. 13 because of the divergence. We observed that the proposed WRDC is robust against road curvature variation and it outperforms the tracking performance of LQR with anti-windup.

5. CONCLUSIONS

This paper has developed a vehicular lateral tracking control scheme with reference redesign to compensate for WRD. A WRDC has been developed in terms of states describing lateral position error on the curved road. The proposed tracking control scheme has been designed by the WRDC gain from the dominant state for the lateral position error in the lane keeping control. By developing the WRDC, state-space reference has been redesigned to achieve sufficient lateral tracking control performance on the curved road. To verify the usefulness of the tracking control, the WRDC applied to the LQR controller has been compared to the standard LQR, LQR with an integrator, and LQR with an anti-windup. The proposed WRDC method was not only robust to transient disturbance but also sufficiently compensates for WRD compared to other methods. The proposed WRDC is expected to improve the vehicular tracking control on the curved road that is very important in autonomous driving vehicles.

REFERENCES

Åström, K.J. and Rundqwist, L. (1989). Integrator windup and how to avoid it. In *1989 American Control Conference*, 1693–1698. IEEE.

Boudali, M., Orjuela, R., and Basset, M. (2019). Unified dynamic and geometrical vehicle guidance strategy to cope with the discontinuous reference trajectory. *Vehicle System Dynamics*, 1–28.

Cao, W., Zhang, J., and Ren, W. (2015). Leader–follower consensus of linear multi-agent systems with unknown external disturbances. *Systems & Control Letters*, 82, 64–70.

Choi, W.Y., Kang, C.M., Lee, S.H., and Chung, C.C. (2017). Waypoint tracking predictive control with vehicle speed variation. In *Proc. Asian Control Conference*, 61–66. IEEE.

Choi, W.Y., Kim, D.J., Kang, C.M., Lee, S.H., and Chung, C.C. (2018). Autonomous vehicle lateral maneuvering by approximate explicit predictive control. In *2018 Annual American Control Conference (ACC)*, 4739–4744. IEEE.

Hu, C., Jing, H., Wang, R., Yan, F., and Chadli, M. (2016). Robust H_∞ output-feedback control for path following of autonomous ground vehicles. *Mechanical Systems and Signal Processing*, 70, 414–427.

Ji, Y. and Chizeck, H.J. (1990). Controllability, stabilizability, and continuous-time markovian jump linear quadratic control. *IEEE Transactions on Automatic Control*, 35(7), 777–788.

Johnson, C. (1971). Accomodation of external disturbances in linear regulator and servomechanism problems. *IEEE Transactions on Automatic Control*, 16(6), 635–644.

Kang, C.M., Lee, S.H., and Chung, C.C. (2014). Lane estimation using a vehicle kinematic lateral motion model under clothoidal road constraints. In *Proc. IEEE International Conference on Intelligent Transportation Systems*, 1066–1071.

Kang, C.M., Lee, S.H., and Chung, C.C. (2018). Discrete-time LPV H_2 observer with nonlinear bounded varying parameter and its application to the vehicle state observer. *IEEE Transactions on Industrial Electronics*, 65(11), 8768–8777.

Kim, D.J., Kang, C.M., Lee, S.H., and Chung, C.C. (2018). Discrete-time integral sliding model predictive control for dynamic lateral motion of autonomous driving vehicles. In *2018 Annual American Control Conference (ACC)*, 4757–4763. IEEE.

Kim, J.S., Kim, D.J., Lee, S.H., and Chung, C.C. (2019). Autonomous driving vehicles with unmatched disturbance compensation using deep neural networks. *International Conference on Control, Automation and Systems (ICCAS)*, 706–711.

Kothare, M.V., Campo, P.J., Morari, M., and Nett, C.N. (1994). A unified framework for the study of anti-windup designs. *Automatica*, 30(12), 1869–1883.

Lee, S.H. and Chung, C.C. (2016). Robust multirate on-road vehicle localization for autonomous highway driving vehicles. *IEEE Trans. on Control Systems Technology*.

Lin, C.F., Ulsoy, A.G., and LeBlanc, D.J. (2000). Vehicle dynamics and external disturbance estimation for vehicle path prediction. *IEEE Transactions on Control Systems Technology*, 8(3), 508–518.

Park, H.G., Ahn, K.K., Park, M.K., and Lee, S.H. (2018). Study on robust lateral controller for differential gps-based autonomous vehicles. *International Journal of Precision Engineering and Manufacturing*, 19(3), 367–376.

Son, Y.S., Kim, W., Lee, S.H., and Chung, C.C. (2015). Robust multirate control scheme with predictive virtual lanes for lane-keeping system of autonomous highway driving. *IEEE Transactions on Vehicular Technology*, 64(8), 3378–3391.

Tunçer, Ö., Güvenç, L., Coşkun, F., and Karsligil, E. (2010). Vision based lane keeping assistance control triggered by a driver inattention monitor. In *2010 IEEE International Conference on Systems, Man and Cybernetics*, 289–297. IEEE.

Van Loon, S., Hunnekens, B., Heemels, W., van de Wouw, N., and Nijmeijer, H. (2014). Transient performance improvement of linear systems using a split-path nonlinear integrator. In *2014 American Control Conference*, 341–346. IEEE.